ELSEVIER

Soil Dynamics and Earthquake Engineering 19 (2000) 115–126

SOIL DYNAMICS AND EARTHQUAKE ENGINEERING

www.elsevier.com/locate/soildyn

Propagation and attenuation characteristics of various ground vibrations

Dong-Soo Kim[a,*], Jin-Sun Lee[1,a]

[a]*Department of Civil Engineering, Korea Advanced Institute of Science and Technology, Taejon, 305-701, South Korea*

Accepted 27 December 1999

Abstract

In order to effectively control vibration related problems, the development of a reliable vibration monitoring system and the proper assessment of attenuation characteristics of various vibrations are essential. Various ground vibrations caused by train loading, blasting, friction pile driving and hydraulic hammer compaction were measured using 3D geophones inside of the borehole as well as on the ground surface, and the propagation and attenuation characteristics of various source generated vibrations were investigated by analyzing particle motions. For the geometric modeling of various vibrations, the types of various sources and their induced waves were characterized and the geometric damping coefficients were determined. The measured attenuation data matched well with the predicted data when using the suggested geometric damping coefficient, and the estimated soil damping ratios were quite reasonable taking soil type of the site and experiencing strain level into consideration.

Keywords: Ground vibration; Attenuation characteristics; Geometric damping; Material damping; Particle motions; Train loading; Blasting; Pile driving; Hydraulic hammer compaction

1. Introduction

Vibrations from construction activities and traffic loading are important because they may cause damage to the adjacent structures as well as complaints to the neighbors. Damage of structures may be caused by the vibration induced differential settlement as well as by vibrations transmitted directly to structures [1–3]. Complexity of these vibrations related problems makes it difficult to identify the causes of damages. For the analysis of vibration related problems, it is necessary to consider the combined effect of several factors such as the characteristics of vibration sources, the site characteristics, the propagation of surface and body waves in the ground, and response of structures [4].

The environmental zone, which is effective to reduce the ground vibration amplitude, is often adopted to prevent the vibration damages. However, it is difficult to estimate to what degree the amplitude of vibration decreases at a certain distance. Generally, the attenuation of vibrations with distance is composed of two factors: geometric damping and material damping. The geometric damping depends on the type and the location of vibration source and the material damping is related with ground properties and vibration amplitude [5].

Most of ground vibrations are currently measured only at the ground surface, not in-depth, without considering the propagation path. Propagation characteristics of vibrations generated by various sources may be dependent on the type of the generated waves, which can be assessed by measuring particle motions in three directions including vertical, longitudinal, and transverse directions. The three directional particle motion monitoring on the ground surface and in-depth is important for the characterization of propagating waves [6].

In this study, the ground vibrations induced by train loading, blasting, friction pile driving, and hydraulic hammer compaction were measured by using 3-component (3D) geophones, which can monitor both surface and in-depth vibrations. By analyzing the measured particle motions and major energy component in the frequency domain, the propagating waves generated by each vibration source was characterized. Finally, attenuation characteristics of vibration sources were investigated considering the source characteristics and the geotechnical properties of the sites.

2. Calibration and development of 3D geophone

For a reliable in-situ vibration measurement, it is the first step to calibrate a vibration monitoring transducer. The

* Corresponding author. Tel.: + 82-42-869-3619; fax: + 82-42-869-3610.

E-mail addresses: dskim@cais.kaist.ac.kr (D.-S. Kim); blueguy@bomun.kaist.ac.kr (J.-S. Lee).

[1] Tel.: + 82-42-869-5659; fax: + 82-42-869-3610.

0267-7261/00/$ - see front matter
PII: S0267-7261(00)00002-6

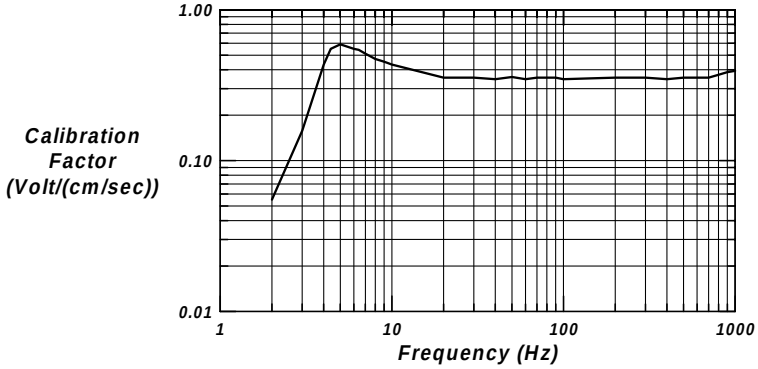

a) Natural Frequency 4.5Hz Vertical Geophone

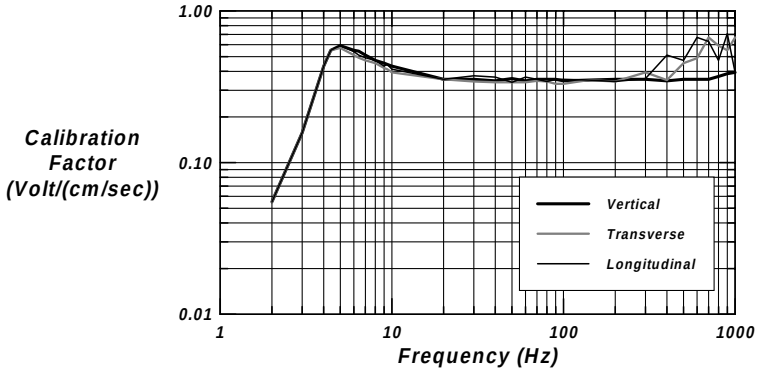

b) 3–Component Geophone

Fig. 1. Calibration curve for 4.5 Hz geophone and 3-component geophone: (a) Natural frequency 4.5 Hz vertical geophone; and (b) 3-component geophone.

velocity transducer, which usually is called geophone, is widely used for ground vibration measurement. The response of velocity transducer becomes nonlinear at low frequencies and has a natural frequency since it is a single-degree-of-freedom system. It is, therefore, necessary to calibrate exact voltage output of the geophone with frequency [7]. Typical calibration curve for the geophone (with open shunt damping) which has a natural frequency of 4.5 Hz is presented in Fig. 1a. Calibration factor is constant in frequencies approximately ranging from 10 to 500 Hz, representing the reliable range of vibration measurement using this transducer. For the vibration measurements at low frequencies below 10 Hz, the 2 Hz geophone (Mark Product L-4) was used with a factory calibration chart.

To characterize the vibrations induced by various sources, it is essential to measure the 3D particle motions. Vibrations are required to be monitored in-depth as well as on the ground surface because some vibration sources such as blasting and pile driving are located at a certain depth below ground. In case of the in-depth vibration measurements, proper orientation and coupling of each transducer in the ground should be secured for the reliable measurements. In this study, 3D-vibration measurement system (3D geophone) was developed by molding three well-calibrated geophones in the aluminum casing in the vertical, longitudinal, and transverse directions. For the in-depth vibration measurements, the 3D geophone can be tightly attached to the borehole at a given depth by inflating a rubber pad, and the direction of each transducer can be confirmed on the ground surface by checking the direction of the orientation rod. The typical frequency responses of the 3D geophone is shown in Fig. 1b, indicating that the vibration measurement can be reliably performed at frequencies ranging from 10 to 200 Hz.

3. Measurement of various ground vibrations

Ground vibrations generated by various sources such as train loading, in-depth blasting, friction pile driving and hydraulic hammer compaction were monitored using the 4.5 and 2 Hz vertical geophones and 3D geophones. The amplitudes in time and frequency domains are analyzed for various ground vibrations.

3.1. Train loading

Monitoring of the ground vibration generated by train loading was performed at the Byung-Jum station in Kyung-Bu railroad using the six calibrated 4.5 Hz vertical geophones and two 3D geophones. The site was composed of 15 m deep residual sandy silt or silty sand layer over weathered rock (Fig. 2a). The locations and spacing of geophones are shown in Fig. 2b. Totally 17 measurements were performed on the ground surface.

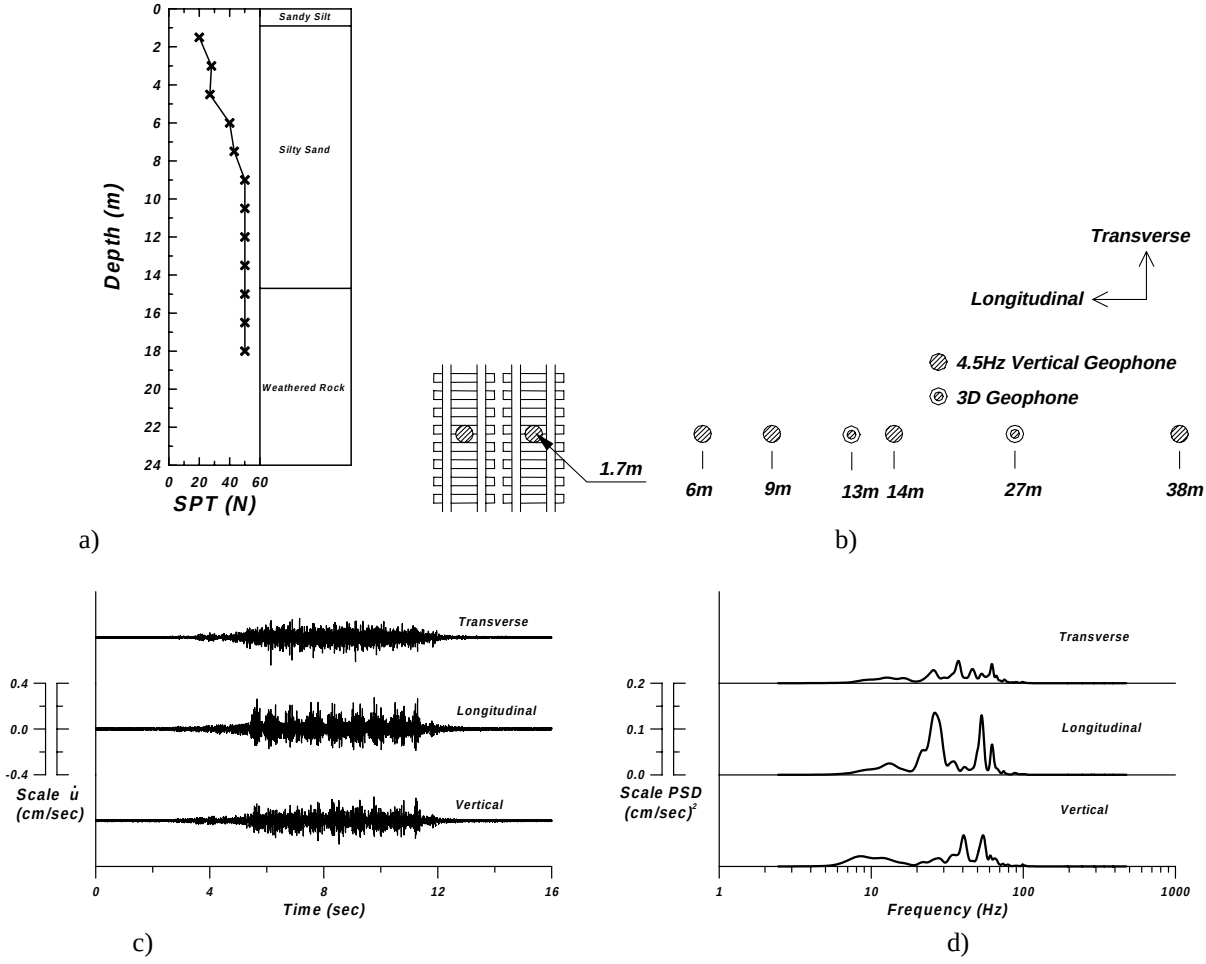

Fig. 2. Site information, typical 3-component time records and power spectral density induced by train. (No. of passenger cars: 8; train speed: 125 km/h; recorded at 13 m apart from sleeper.)

The vibration amplitude measured on the adjacent ground was reduced to about 2 cm/s due to the effect of ballast whereas the amplitude on the sleeper was about 10 cm/s. The vibration amplitude usually increases as increasing the train speed. Typical time domain signals measured using 3D geophone located 13 m apart from the sleeper are shown in Fig. 2c. The energy generated by train induced vibration exist in all three directions almost evenly.

The dominant frequency ranges induced by train loading can be represented by the sleeper passing frequency and the wheel passing frequency [8]. As shown in Fig. 2d, the train induced frequency measured on the ground was widely distributed in the ranges from 7 to 70 Hz. The dominant frequency range varies a little depending on the train speed.

3.2. Blasting

Test blasting before major tunnel construction for high-speed railroad was performed and blasting induced vibrations were measured at Taejon. The test site was composed of 12 m depth fill and weathered soil layer over weathered rock (Fig. 3a). Blasting was performed inside the bedrock at depths of about 28–44 m using $1 \sim 3$ kg charge weight. Vibrations were measured in-depth as well as on the ground using three 4.5 Hz vertical geophones and two 3D geophones as shown in Fig. 3b. The peak particle velocity varies significantly due to the charge weights and the measured value at a horizontal distance of about 32 m was in the range from 1.5 to 2.5 cm/s.

Typical time domain signals measured by a 3D geophone at a depth of 7.5 m are presented in Fig. 3c. Depending on the orientations of transducers, either P or S wave energy was dominant: in the longitudinal and vertical direction the P wave was dominant whereas S wave energy was bigger in the transverse directions. Vibration amplitude was a little bigger in the vertical and longitudinal direction than in the transverse direction. Most of the energy in the blasting induced vibration exists at frequencies below about 50 Hz, and the spectrum energy in the longitudinal direction was larger than others as shown in Fig. 3d.

3.3. Friction pile driving

Vibrations caused by friction pile driving were measured

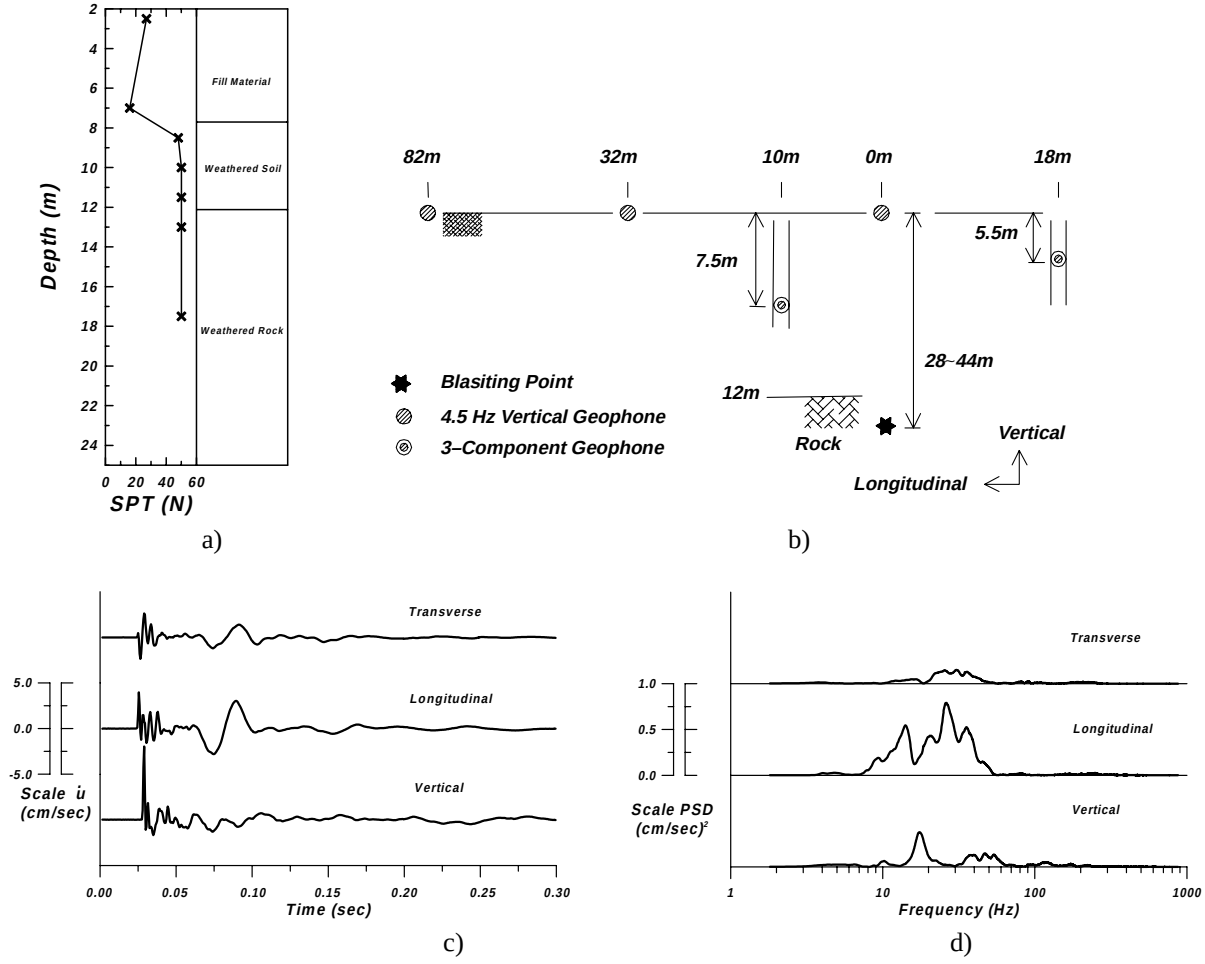

Fig. 3. Site information, typical 3-component time records and power spectral density induced by in-depth blasting. (Charge weight: 2 kg TNT; depth of explosion: 28 m, recorded at distance 10 m, 7.5 m, horizontal and depth, respectively.)

at a long-span bridge pier construction site located at Pusan. The steel pipe pile (diameter of 0.6 m) was driven to the depth of about 40 m using hydraulic hammer with a hammer weight of 7 t and a drop height of 0.8 m. The site was composed of 15 m of gravel fill, interbedded medium silty sand and clay layers of about 20 m, sand layer 5 m, weathered residual soil layer of 7 m and bedrock (Fig. 4a). During driving at tip depths of 16 ~ 28 m, vibrations were measured using three 4.5 Hz vertical geophones and two 3D geophones as shown in Fig. 4b.

The peak particle velocity decreases as increasing the depth to the pile tip and the amplitude measured on the ground surface at a distance of about 7 m ranges from 0.15 to 0.5 cm/s. Typical time and frequency domain signals measured by a 3D geophone at a depth of 15 m are presented in Fig. 4c and d. Most of the energy in the friction pile induced vibration was transmitted by vertical motion with frequencies below about 10 Hz except transverse motion. At a given horizontal distance, the magnitudes of vertical particle motions measured on the ground surface and at depth of 15 m were almost identical. It appears that friction pile driving tries to overcome the friction mobilized between soil and pile shaft, and during this process a whole mass of soil layer vibrates at low frequencies.

3.4. Hydraulic hammer compaction

Hydraulic hammer compaction was performed at Yongjong Island where Inchon International Airport being constructed. The site consisted of a reclaimed soil of about 6 m and a weak alluvial clayey silt layer of about 20 m and an alluvial stiff silty clay layer of about 15 m, residual sandy soil and bed rock (Fig. 5a). The reclaimed layer, classified as SM, was required to be improved to build a pavement structures for run way, taxiway and apron. The hydraulic hammer compaction with a tamper of 10 t and a drop height of 1.2 m was employed to improve the reclaimed layer minimizing the size of the disturbed craters. Vibrations were measured using four 2 Hz vertical geophones and two 3D geophones as shown in Fig. 5b.

The peak particle velocity measured at distances about of 10–100 m ranges from 0.1 to 4 cm/s. Typical time domain signals monitored on the ground surface by using 3D geophone are shown in Fig. 5c. The vibration amplitude

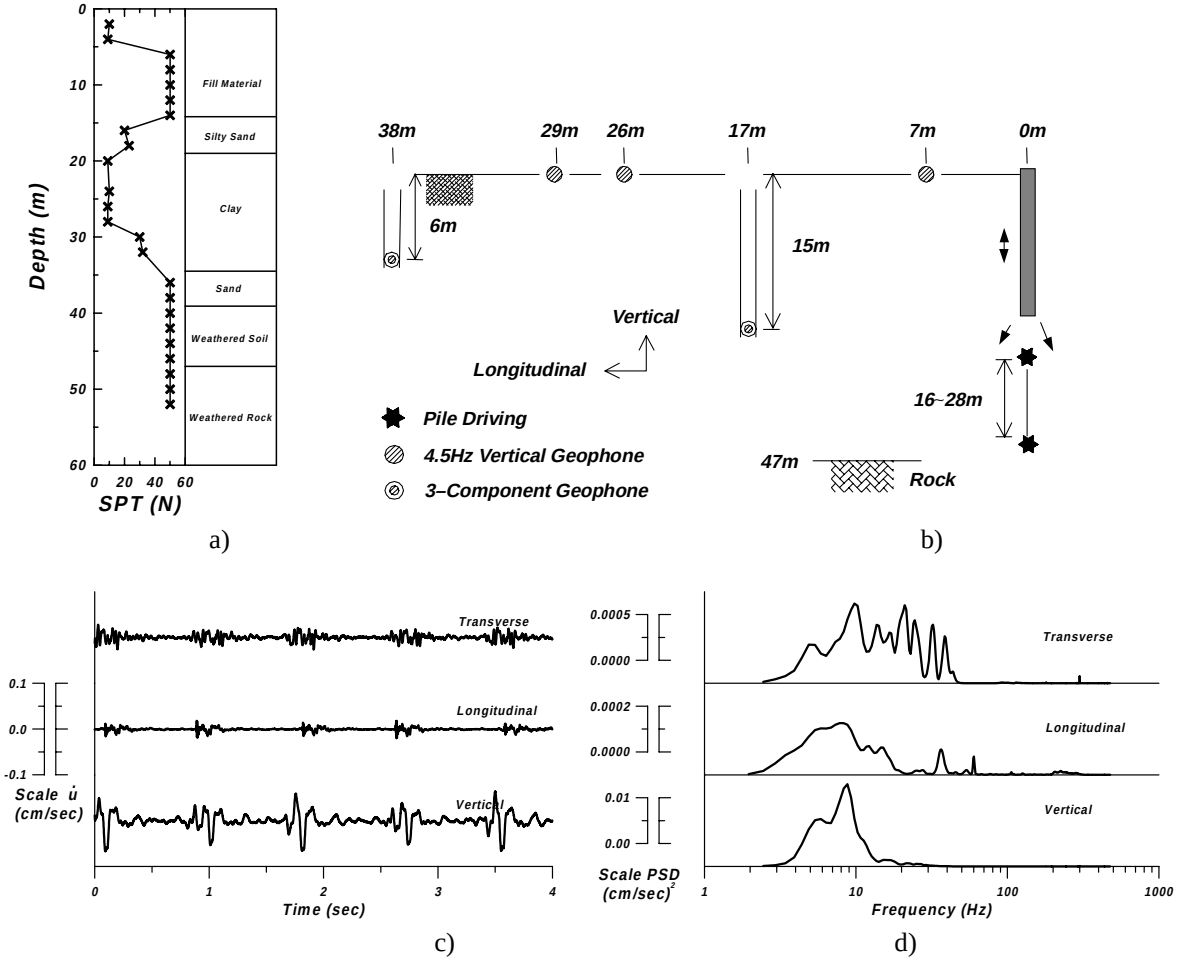

Fig. 4. Site information, typical 3-component time records and power spectral density induced by friction pile driving. (Depth of pile tip: 17 m; recorded at distance 17 m, 15 m, horizontal and depth, respectively.)

in the vertical direction was largest and the amplitudes in the longitudinal and transverse directions were about 75 and 35% of the vertical amplitude, respectively. The most of the energy induced by compaction exists in frequencies of 3–10 Hz for the vertical and longitudinal motions, and some energy exists above 10 Hz for the transverse motion (Fig. 5d).

4. Propagation and attenuation of various ground vibrations

Propagation characteristics of vibrations generated by various vibration sources may be dependent on the type of the generated waves which can be assessed by measuring particle motions. Vibration amplitude is reduced during their propagation through the ground because of geometric and material dampings. To therefore effectively control the vibration related problems, the investigations of propagation and attenuation characteristics are required.

4.1. Theoretical background of vibration attenuation

Vibrations lose energy during propagating in the ground and the amplitude of the vibrations decreases with increasing distance from the source. The decay of amplitude of vibration with distance can be attributed to two components; geometric (radiation) damping and material damping, which may be described by the following equation [9]

$$w_2 = w_1\left(\frac{r_1}{r_2}\right)^n \mathrm{e}^{-\alpha(r_2-r_1)} \tag{1}$$

where, w_1 and w_2 are vibration amplitudes at distance r_1 and r_2 from a source of vibration; n is a geometric damping coefficient; α is a material damping coefficient.

The geometric damping occurs due to the decrease of the energy density with distance from source. Geometric damping coefficient can be analytically determined by assessing the type of the propagating wave, source type and location as shown in Table 1 [10]. Geometric damping occurs even in a perfectly elastic media.

Meanwhile, the ground is not perfectly elastic and the

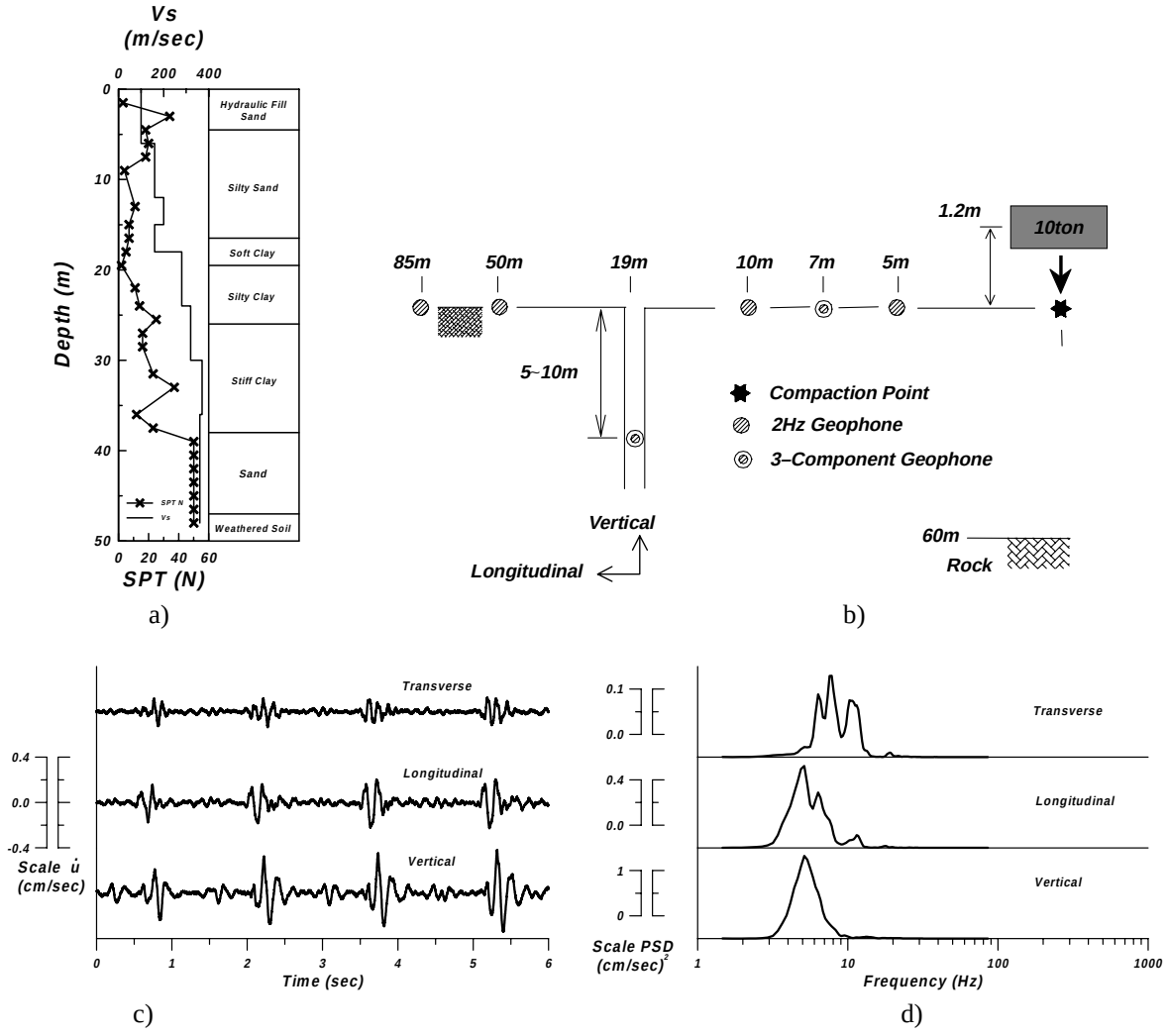

Fig. 5. Site information, typical 3-component time records and power spectral density induced by hydraulic hammer compaction. (Recorded at horizontal distance 7 m.)

vibration energy is reduced due to the friction and cohesion between soil particles. This attenuation due to material damping is affected by the soil type and frequency of vibration. Material damping coefficient, α, can be represented as:

$$\alpha = \frac{\pi \eta f}{c} \tag{2}$$

where η is a loss factor, f is a frequency of the wave and c is the propagation velocity of the wave. Woods and Jedele [5] classified the site soils into four classes ranging from sound, hard rock to weak and soft soils. The loss factor is related with the hystertic damping ratio of the ground. Because the damping ratio is constant and minimum below the elastic threshold strain and then increases with increasing strain

Table 1
Geometric damping coefficients for various sources [10]

Physical sources	Type of source	Wave	Location	n
Highway/Rail line footing array	Line	Surface	Surface	0
		Body	Surface	1.0
Car in pothole, Single footing	Point	Rayleigh	Surface	0.5
		Body	Surface	2.0
Tunnel	Buried Line	Body	Interior	0.5
Buried explosion	Buried point	Body	Interior	1.0

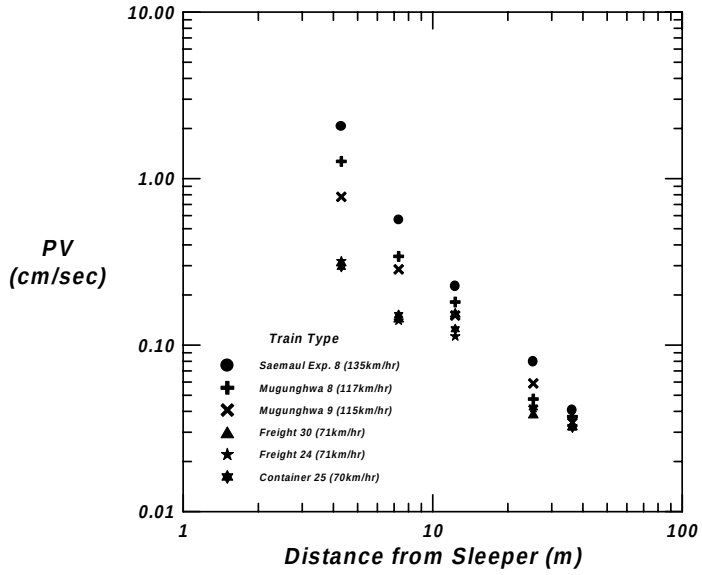

Fig. 6. Attenuation characteristics with distance of various train loading.

amplitude [11], the material damping coefficient is also affected by the strain amplitude of ground experiencing by propagating vibrations, which can be expressed by the following equation:

$$\gamma = \frac{\dot{u}}{v_s} \tag{3}$$

where γ is shear strain, $\dot{u}$ is particle velocity and v_s is shear wave velocity.

4.2. Propagation and attenuation characteristics of train induced vibration

The train induced vibration is generated by moving load. The vibration measured at a certain distance from the rail is a superposed signal of various vibrations occurred at different locations with different phases. These characteristics affect the propagation and attenuation characteristics of train induced vibrations. The variations in vibration amplitude with distance for various types of trains are shown in Fig. 6. It is interesting to note that the speed and length of train affect the vibration amplitude and the rate of attenuation.

Gutowski and Dym [10] have mentioned that a train can be modeled as a line source if the distance of the receiver is less than $1/\pi$ times the source length, and the major energy is transmitted in Rayleigh wave form with no geometric damping. In this study, the length of train ranges from 130 to 450 m and the distance to the farthest receiver is 38 m, which exists within $1/\pi$ times the source length. The measured attenuation rate in Fig. 6 was far greater compared with their reasoning.

In order to assess the characteristics of propagating wave, variation in particle motion with time history was detected using the recorded data from the 3D geophone. As shown in Fig. 7, train induced vibration was mainly composed of Rayleigh wave with elliptic counter-clockwise motion. However, significant amount of horizontal shear wave energy portion was shown in vertical–transverse plane. The train induced vibration was found to contain 3-directional motions almost evenly, and can be characterized as a mixture of body and surface waves. Therefore, it is hard to

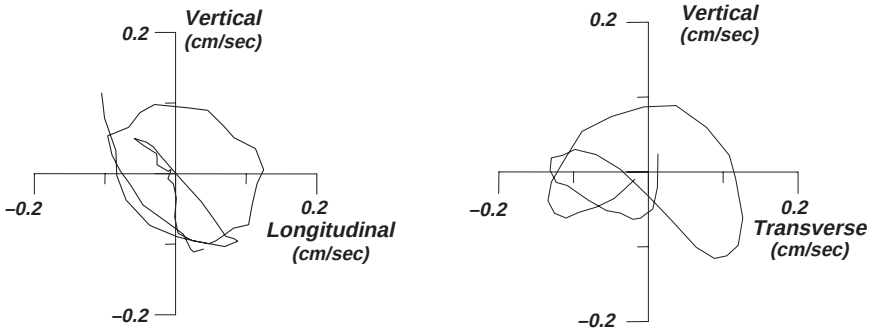

Fig. 7. Particle motion of train induced vibration.

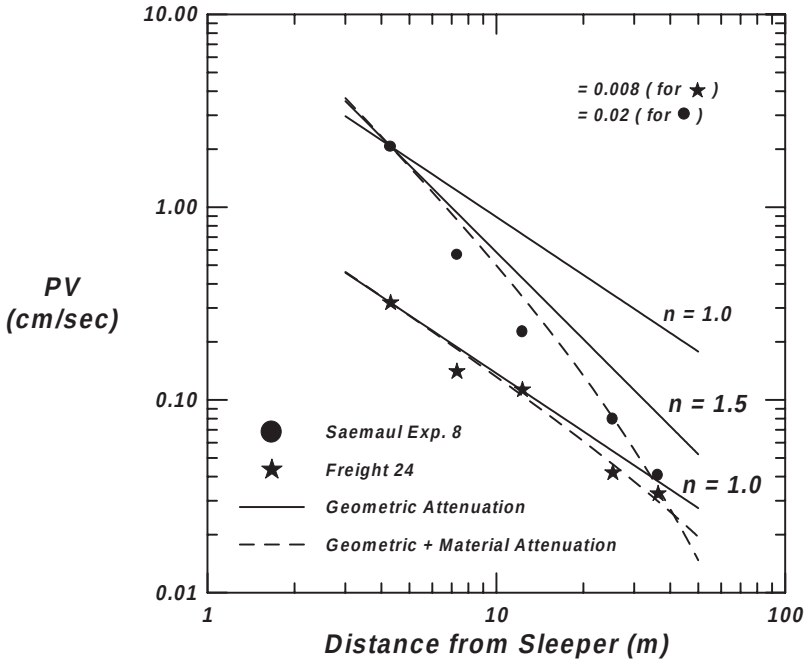

Fig. 8. Attenuation with distance of train induced vibration.

select the geometric attenuation coefficient of train induced ground vibration, and Verhas [12] has introduced a superposed attenuation model. But the superposed model was too site specific and the resulting material damping ratio of soil was about 5–7% which was relatively high where the soil undergoes linear deformation ranges.

In order to investigate the effects of the speed and length of train on the attenuation characteristics, the variations in vibration amplitude with distance are plotted in Fig. 8 for two cases: (i) a saemaul express train of 8 cars with a speed of 135 km/h; and (ii) a freight train of 24 cars with a speed of 71 km/h. Ground vibration induced by shorter and faster train was attenuated faster than that of longer and slower train. Due to the superposition effect of moving load, train loading of the shorter and faster train can be characterized as a combination of the point and the line sources of body wave with a geometric damping coefficient of 1.5. If this loading was classified as a point source, the geometric attenuation would be larger than measured attenuation, whereas if classified as a line source, the material damping would be unreasonably high. For the longer and slower train, it can be characterized as a line source of body wave with a geometric damping coefficient of 1.0. The material damping coefficients of the site of the faster train and the slower train were evaluated as 0.02 and 0.008 (1/m), respectively. The corresponding damping ratio and the maximum strain amplitude were 2.3 and 0.01% for the faster train, and 0.9 and 2×10^{-3}% for the slower train. The calculated damping ratio was reasonable considering the soil type and the experiencing strain amplitude. If the train induced vibrations were classified as Rayleigh wave, the corresponding soil damping ratio to meet the attenuation characteristics should be unrealistically high.

4.3. Propagation and attenuation characteristics of blasting induced vibration

Ground vibration generated by in-depth blasting propagates

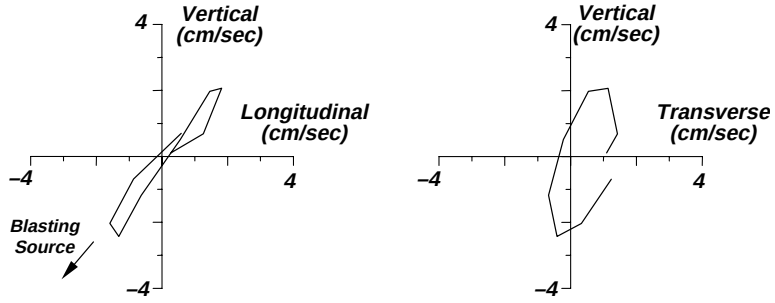

Fig. 9. Particle motion of in-depth blasting induced vibration.

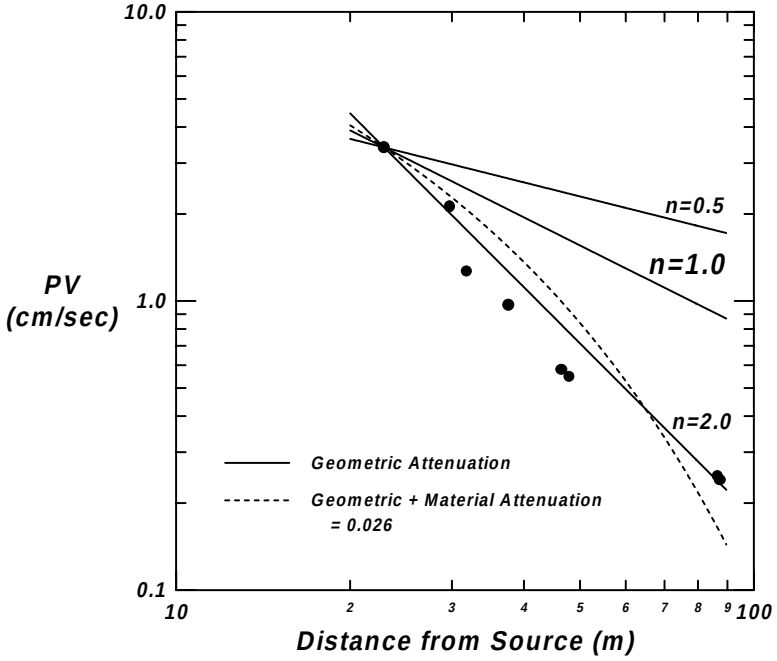

Fig. 10. Attenuation with distance of in-depth blasting induced vibration.

through rock or soil layer. If the layer is composed of several different types of soil, the transmission path of the blasting vibration is very complicated because of the reflection and refraction of the waves. In order to evaluate the major energy component of blasting induced vibration, the variations in particle motions in the vertical–longitudinal and vertical–transverse planes are plotted in Fig. 9. It can be clearly noticed that the compression wave components in the direction of source to receiver arrived dominantly. Therefore, blasting can be classified as an in-depth point source, which generates the P-waves and the propagation distance can be estimated as a distance from the source with a spherical wavefront. Typical variation in particle velocity of blasting induced vibration with distance is shown in Fig. 10. The measured attenuation data matched well with the geometric damping coefficient of 1.0 which represents body wave generated by the in-depth point source and the material damping coefficient of 0.026 (1/m). The corresponding damping ratio was 4–5% which was reasonable at a maximum strain amplitude of about 0.01% where the site soil experienced.

4.4. Propagation and attenuation characteristics of friction pile driving

It is generally considered that waves emanating from source such as a pile in the ground will include elastic waves in the form of compression waves, shear wave, and surface waves. Compression waves are considered to propagate from the area of the pile toe, expanding outwards over a spherical wavefront with a geometric damping coefficient of 1.0. The vertical shear waves emanates from shaft friction and expanding around a conical surface [13]. These concepts are shown in Fig. 11.

The variations in particle motions with time are shown in Fig. 12. Particle motions are mostly in the vertical direction,

Table 2
Geometric damping coefficients for various sources used in this study

Vibration sources used in this study	Location/Type of source	Induced wave type	*n*
Short length and high speed train	Surface/Combination of point and infinite line	Body wave	1.5
Hydraulic compaction	Surface/Point	Surface wave	0.5
Long length and slow speed train	Surface/Infinite line	Body wave	1.0
In-depth blasting friction pile driving	In-depth/Point	Body wave	1.0

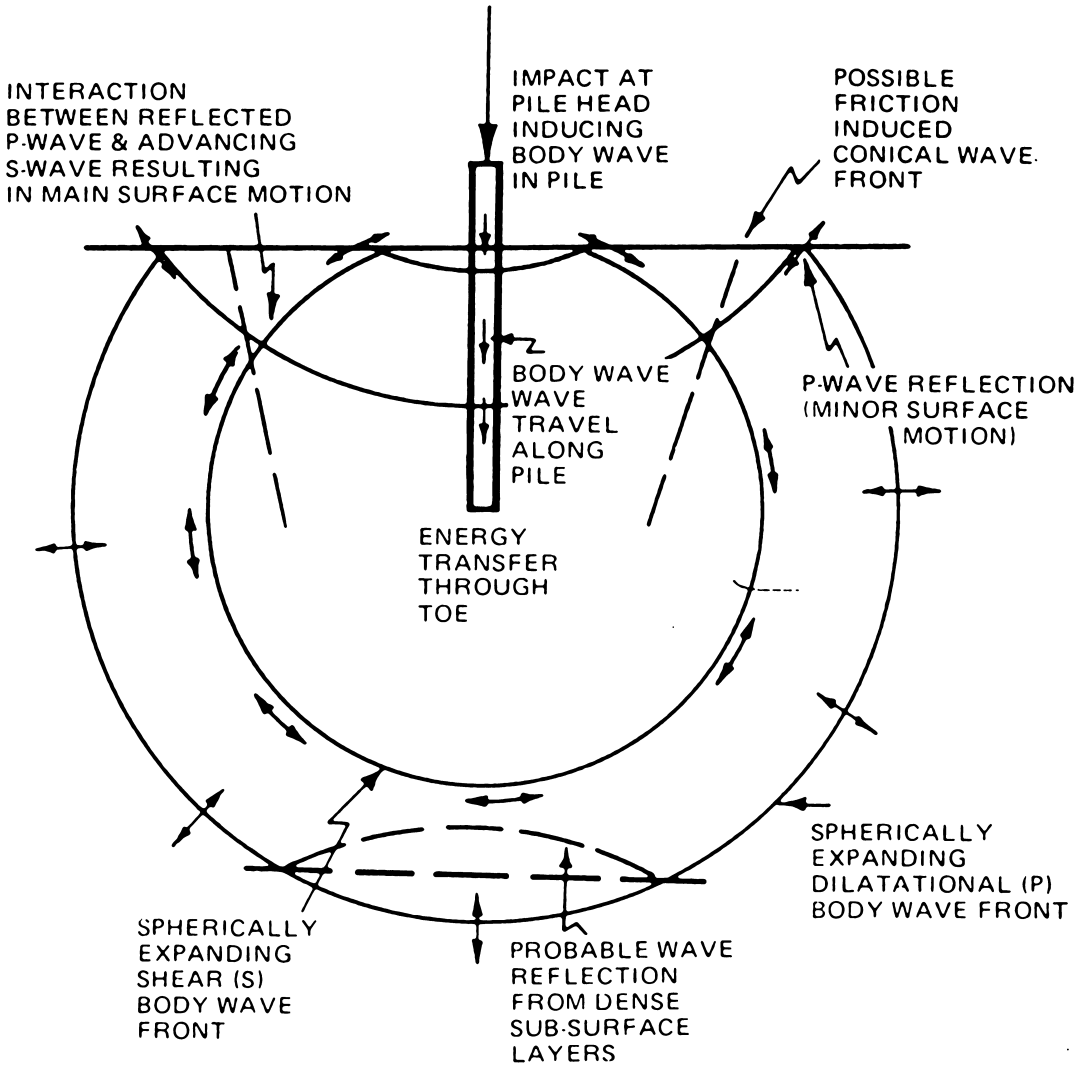

Fig. 11. Possible wavefronts from a driven pile [13].

and vibrations generated by friction pile driving can be characterized as a vertical shear wave with a conical wavefront. Therefore, the source can be classified as a point source generating body wave and the travel distance can be estimated as a horizontal distance from the source. Typical attenuation characteristics of the vibrations generated by friction pile driving are shown in Fig. 13. Using the geometric damping coefficient of 1.0 representing the in-depth point source, the measured characteristics matched well with the α value of 0.026 and the corresponding damping ratio of the site is 5–6% which is a little high at a maximum strain amplitude of about 0.001%. With the

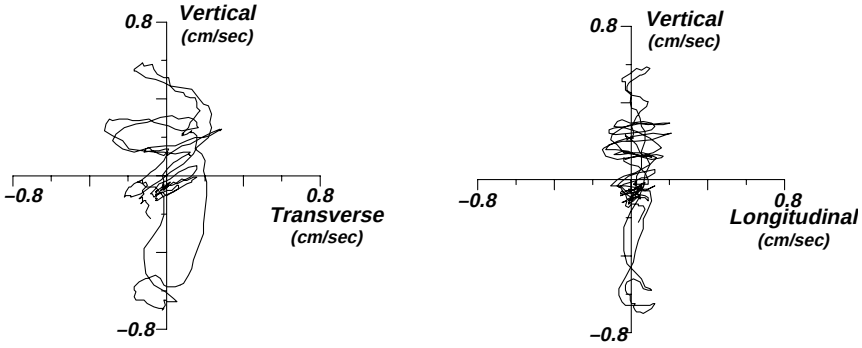

Fig. 12. Particle motion of friction pile driving induced vibration.

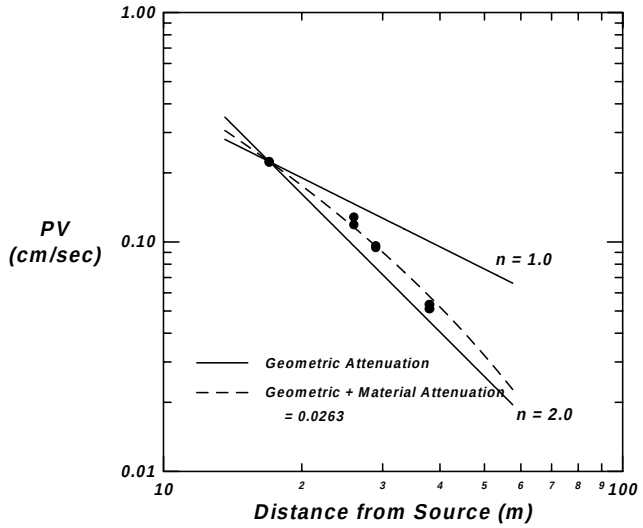

Fig. 13. Attenuation with distance of friction pile driving induced vibration.

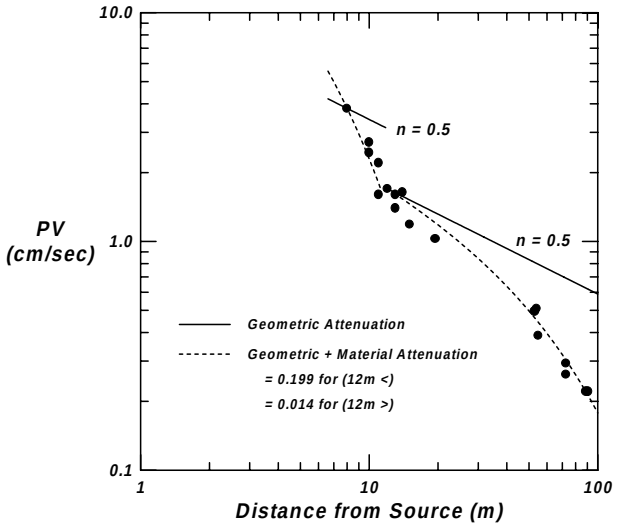

Fig. 15. Attenuation with distance of hydraulic compaction induced vibration.

geometric damping coefficient of 2.0 representing the surface point source, geometric damping exceed actual attenuation data.

4.5. Propagation and attenuation characteristics of hydraulic hammer compaction

The hydraulic hammer compaction, which is similar to vertically vibrating footing may generate both the body waves with a hemispherical wave front and the surface wave with a cylindrical wave front. [14]. The particle motions plotted in the vertical–longitudinal and vertical–transverse planes indicates that the major vibrating energy is transmitted by the surface wave with a retrograde ellipse particle motion (Fig. 14). The source can be classified as a surface point source generating surface wave and the travel distance can be estimated as a surface horizontal distance from the source.

The typical attenuation of particle motion with distance is shown in Fig. 15. The attenuation characteristics were predicted by using the geometric damping coefficient of 0.5, which is for the case of a surface point source generating the surface wave. The corresponding α values can be estimated separately as 0.199 in the near field within 12 m and 0.014 in the far field beyond 12 m. The wavelength of the propagation wave is about 12 m. The corresponding damping ratio in the near field was about 40% at the strain amplitude of 0.05% and the damping ratio in the far field was about 3% at strain amplitude of about 0.004%. Taking the soil type of the site and the experiencing strain level into consideration, the estimated damping ratios in the far field is reasonable, but the damping ratio in the near field is quite high. In the near field within the distance of one wavelength, body wave energy is significant and cannot be ignored in the estimation of geometric attenuation coefficient [15]. Therefore, the reason of high damping ratio can be explained by the body wave propagation in the near field which did not counted in the estimation of geometric attenuation coefficient.

5. Conclusions

Propagation and attenuation characteristics of various

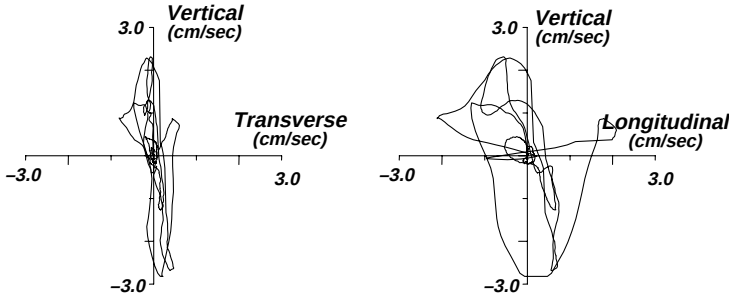

Fig. 14. Particle motion of hydraulic compaction induced vibration.

vibrations generated by train loading, blasting, friction pile driving, and hydraulic hammer compaction were investigated and the following conclusions can be drawn for this study.

1. Monitoring of particle motions using 3D geophones inside of the borehole as well as on the ground surface was effective to determine the propagation path and the type of major waves generated by various sources.
2. The train induced vibration was a mixture of body and surface waves and the primary energy of blasting induced vibration was transmitted by a compression wave. Friction pile driving provides a dominant vertical shear wave with a conical wave front and for a hydraulic hammer compaction major energy is transmitted by the surface wave with a retrograde elliptic particle motion.
3. For the geometric modeling of various vibrations, the types of source and induced wave are required to characterize. Train loading can be modeled as either a point or a line source depending on its length and speed which generating body wave. The in-depth blasting can be modeled as a body wave generating point source, the friction pile driving as a body wave generating point source, and hydraulic hammer compaction as a surface wave generating point source. The corresponding geometric damping coefficients are summarized in Table 2.
4. The measured attenuation data matched well with the predicted data when using the suggested geometric damping coefficient, and the estimated damping ratios were quite reasonable taking soil type of the site and experiencing strain level into consideration.

Acknowledgements

This work was partially supported by the KISTEP(ED-01-04) and KEERC(97KS-1031-02-03-3). This support is gratefully acknowledged.

References

[1] Kim DS, Drabkin S. Investigation of vibration induced settlement using multifactorial experimental design. Geotechnical Testing Journal, GTJODJ 1995;18(4):463–71.
[2] Kim DS, Drabkin S, Rokhavarger A, Laefer D. Prediction of low-level vibration induced settlement, Geotechnical special publication, 40. New York: ASCE, 1994. p. 806–17.
[3] Drabkin S, Lacy H, Kim DS. Estimating settlement of sand caused by construction vibration. Journal of Geotechnical Engineering 1996;122(11):920–8.
[4] Massarsch KR. Man-made vibrations and solutions. Proceedings of the Third International Conference on Case Histories in Geotechnical Engineering. St. Louis, Missouri, 1993. p. 1393–405.
[5] Woods RD, Jedele LP. Energy attenuation relationships from construction vibrations. Vibration Problems in Geotechnical Engineering. ASCE Convention in Detroit, Michigan, 1985. p. 229–46.
[6] Taniguchi E, Sawada K. Attenuation with distance of traffic-induced vibrations. Soil and Foundations 1979;19(2):16–28.
[7] Lam Y. Laboratory evaluation of geophone performance at high frequencies. MSCE dissertation. The University of Texas at Austin, 1989.
[8] Heckel M, Hauck G, Wettschureck R. Structure-borne sound and vibration from rail traffic. Journal of Sound and Vibration 1996;193(1):175–84.
[9] Bornitz G. Über die Ausbreiting der von Groszkolbenmaschinen erzengten Bondenschwingungen in die Tiefe. Berlin: Springer, 1931.
[10] Gutowski T, Dym C. Propagation of ground vibration: a review. Journal of Sound and Vibration 1976;49(2):179–93.
[11] Kim DS, Stokoe KH. Torsional Motion monitoring system for small-strain (10^{-5} to 10^{-3}%) soil testing. Geotechnical Testing Journal, GTJODJ 1994;17(1):17–26.
[12] Verhas HP. Prediction of the propagation of train-induced ground vibration. Journal of Sound and Vibration 1979;66(3):371–6.
[13] Attewell PB, Farmer IW. Attenuation of ground vibrations from pile driving. Ground Engineering 1973;6(4):26–9.
[14] Richart FE, Hall JR, Woods RD. Vibration of soils and foundations. Englewood Cliffs, NJ: Prentice-Hall, 1970.
[15] Sanchez-Salinero I. Analytical investigation of seismic methods used for engineering applications. PhD dissertation. University of Texas at Austin, 1987.